

LATERAL ROTATION AND FLIGHT DYNAMICS OF A RECOVERABLE SUB-ORBITAL PLATFORM

Victor Koldaev – koldaev@iae.cta.br

Paulo Moraes Junior – moraes@iae.cta.br

Instituto de Aeronáutica e Espaço, Centro Técnico Aeroespacial, Divisão de Sistemas Espaciais, 12228-904, São José dos Campos, SP, Brasil

***Abstract.** Returnable sub-orbital or orbital platforms need measurement conditions improvement and safe recovery system. To improve microgravity environment and to minimize flight loads of such vehicles a stable platform motion is desired. The lateral load determination during re-entry makes necessary to simulate the platform rotation around its center of gravity. This work discusses the modeling aspects of the platform separation from rocket booster and its lateral rotation (pitch and yaw planes) in a sub-orbital flight. The programs for the simulation of rotation are suggested. An analysis of the sub-orbital trajectory for the recoverable platform SARA was conducted. The simulation gives detailed information on the microgravity during the flight in the outer atmosphere. It has been shown that the application of a special restrainer during the platform separation from booster can improve the microgravity environment. The platform rotation at high altitudes can cause oscillation with a long settling time. High lateral components of aerodynamic forces can occur due to great amplitudes of the angle of attack during the platform deceleration in the lower atmosphere. The platform orientation and rotation at parachute opening moment have been determined. Dynamics simulation of the platform with some parachutes during the system descent is presented.*

***Keywords:** Recoverable platform, Sub-orbital flight, Rotation dynamics.*

1. INTRODUCTION

Future space exploration exhibits a significant demand for return of materials processed in space and quick access to the samples by users, which can be best accomplished by recoverable platforms. The process of design of such vehicles needs the development of models and numerical techniques to predict platform dynamics during the system motion.

A good concept and design lead to maximization of performance and, consequently, to weight minimization of the complete system, which is of great importance for space systems (Deweese, Schultz & Nutt, 1978, Yaroshevsky, 1988). The recoverable platform technology was benefited from rapid improvement in the rigor of modeling of processes and analytical methods of calculation made possible and practical by development of complex and flexible computer programs. While dynamics simulation are still of major importance to the design process, the facility with which system and component designs can be executed and analyzed, their performance predicted, and test data reduced and evaluated has both speeded the design process and improved depth and quality of results. A number of different programs for dynamics simulation of such systems are developed now in great detail (Rysev etc., 1994, Moraes, 1998, Koldaev etc., 1999).

2. RECOVERABLE SUB-ORBITAL VEHICLE

An orbital platform will be used to perform microgravity experiments in orbit (Moraes, 1998), and its recovery must be safe and soft, in order to protect the payload from high water or ground impact. Figure 1 shows schematically the procedure of sub-orbital flight, re-entry in the earth atmosphere and sea splash down of such platform.

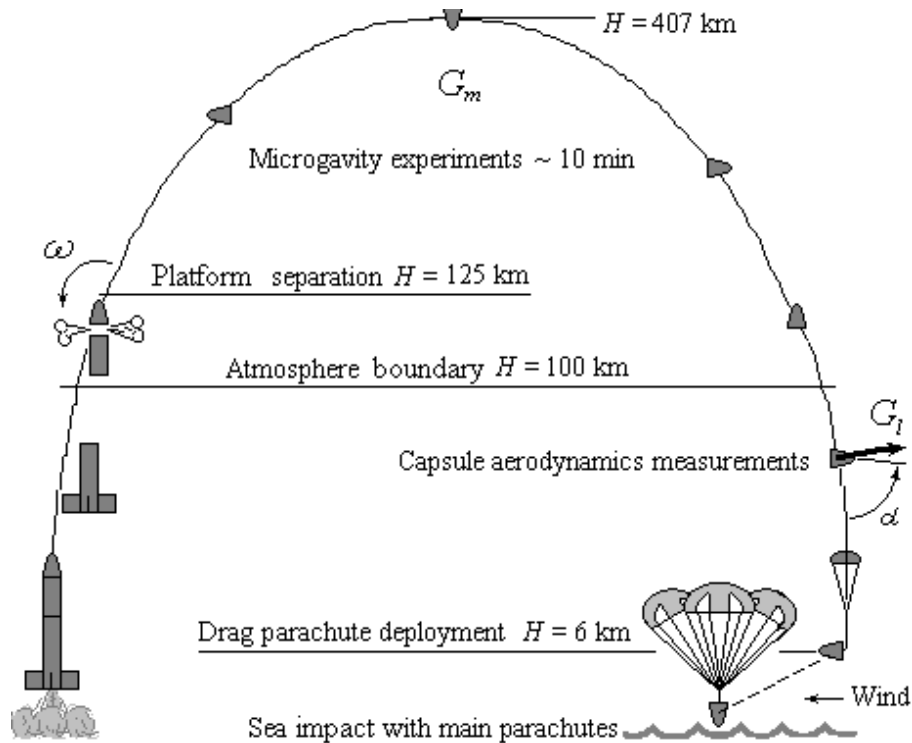


Figure 1 – Flight of the recoverable platform SARA Sub-orbital

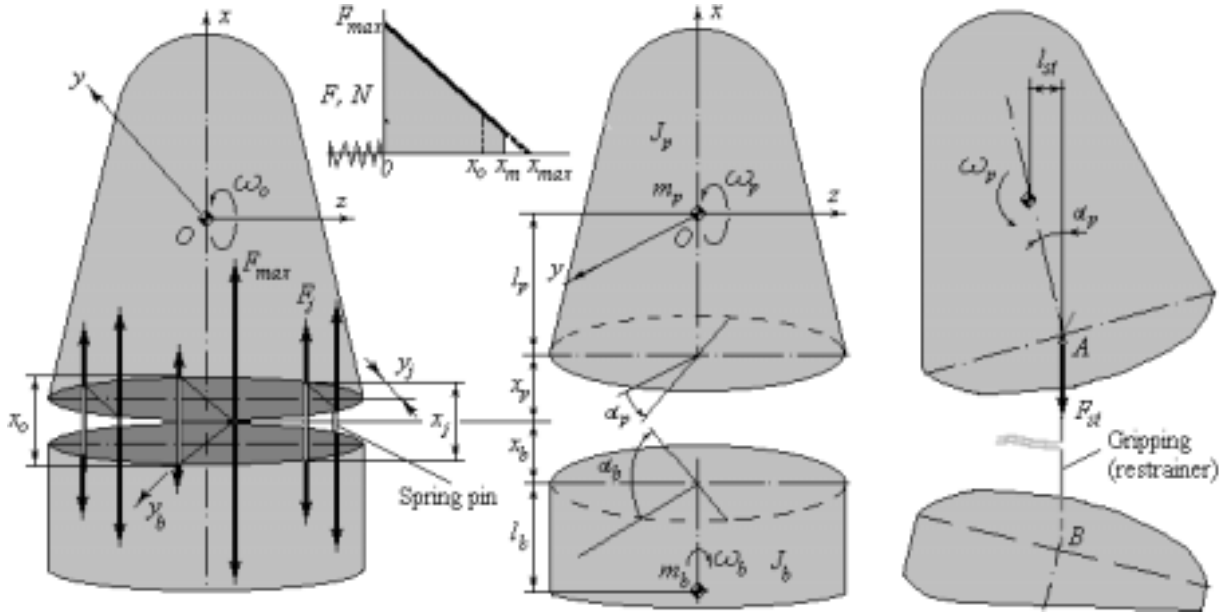
The specification for the altitude of the platform separation depends on the booster burning time and conditions of experiments. For platform SARA Sub-orbital (Fazolli, 1999), the separation from the booster takes place at the altitude of approximately 125 km beyond the atmosphere boundary, where the aerodynamics influence is absent. The platform acceleration due to lateral rotation during the sub-orbital flight at altitudes $H > 100$ km must be kept very small in order to realize a good microgravity environment.

During re-entry in the atmosphere, the platform is stabilized with great values of axial and lateral accelerations. After re-entry, the capsule shaped platform will decelerate to subsonic velocities. At 6 km altitude, the velocity of the platform is approximately 120 – 140 m/s, so that the recovery system, based on drag and main parachutes, can be put in action, bringing in this way the platform to sea surface with velocity of approximately 10 m/s (Moraes, 1998).

3. MODELING OF PLATFORM SEPARATION

Unrestricted motion of the platform out of atmosphere starts after its separation from the booster (Figure 1). Within this, the lateral rotation intensity and the corresponding centripetal acceleration are determined by the repulsion impulse asymmetry, which depends on the separation equipment design. Usually, such a mechanism consists of pyrotechnic actuators,

which, at the moment of putting them into action, releases the springs, located along the joint outline of the platform with the booster. The last ones are pushed apart with the help of spring pins (Figure 2a).



a – initial spring forces

b - motion parameters

c – restrainer scheme

Figure 2 – Separation dynamics of SARA Sub-orbital platform from rocket booster

As it is impossible to obtain absolute simultaneity and symmetry of the pyrotechnic actuators operating and the spring release, then, the platform skewing with the offset x_0 is possible. Offset value x_0 can be limited with the help of a guide mechanism (if it possible) and is used as the initial condition parameter for the spring action.

Distance y_j is determined by the platform design and can be taken as a constant value during separation. For the outer atmosphere motion, the equations of rotation during the platform separation have the form

$$m_p \frac{d^2 x_p}{dt^2} = \sum F_j, \quad j = 1, 2, 3, \dots, N \quad (1)$$

$$m_b \frac{d^2 x_b}{dt^2} = - \sum F_j, \quad j = 1, 2, 3, \dots, N \quad (2)$$

$$J_p \frac{d\omega_p}{dt} = \sum F_j y_j, \quad j = 1, 2, 3, \dots, N \quad (3)$$

$$J_b \frac{d\omega_b}{dt} = - \sum F_j y_j, \quad j = 1, 2, 3, \dots, N \quad (4)$$

where x_p and x_b displacements of platform and booster from initial point, m
 y_j distance from platform surface XOZ to actuator (Fig. 2a), m
 J_p and J_b inertia moment of platform and booster, kg m²
 ω_p and ω_b rotation rate of platform and booster, rad/s
 N number of actuators.

One can determine the angles of orientation (Fig. 2b), in the form of the finite differences

$$\alpha_{pi+1} = \alpha_{pi} + \omega_{pi} \Delta t + (d\omega_{pi}/dt) \Delta t^2 / 2 \quad (5)$$

$$\alpha_{bi+1} = \alpha_{bi} + \omega_{bi} \Delta t + (d\omega_{bi}/dt) \Delta t^2 / 2 \quad (6)$$

where α_p and α_b angles of platform and booster orientation, m.

If one takes $x_{j=1} = 0$ for neighboring points of platform and booster, then, it is possible to write the parameters of initial position as

$$\begin{aligned} x_p(0) &= R \sin \alpha_p \\ x_b(0) &= R \sin \alpha_b \\ x_p &= 2R \sin (\alpha_p + \alpha_b) \end{aligned} \quad (7)$$

where R radius of platform, m.

The spring forces, F_j , depend on the displacement x_j during the relative motion and rotation of the platform and the booster. The value F_j (Fig. 2a), can be determined as

$$F_j = k (x_{max} - x_j) = F_{max} (1 - x_j/x_{max}) \quad (8)$$

where k spring ratio, N/m

F_{max} initial (maximum) spring force, N

x_{max} maximum spring compression, m .

Displacement of the contact points in the case of small turning depends on relative displacement and orientations of the platform and booster

$$x_j = x_p + x_b + y_j \sin (\alpha_p + \alpha_b) \quad (9)$$

Due to sequence of events, which the mathematical modeling intends to capture, an explicit method of solution of the equations (1)-(4) was chosen. Multistep-method type was used for the temporary discretization. This allows to control easily the size of the step in the time level. Temporary integration of the equations is calculated in the known way (Babuska et al, 1966).

The calculation of SARA platform rotation during its separation from the booster of vehicle VS-40 with use of SEPAR program has been done for parameters $R = 0.5$ m, $m_p = 215$ kg, $J_p = 225$ kg m², $N = 12$, $F_{max} = 410$ N, $x_{max} = 27$ mm, $x_m = 25$ mm, $m_b = 178.5$ kg, $J_b = 51.75$ kgm² with initial conditions: $\alpha_b(0) = 0$, $\omega_b(0) = 0$, $dx_{pi}/dt(0) = 0$, $\omega_p(0) = 0$, $dx_b/dt(0) = 0$. The result of calculation versus initial platform offset is shown in Fig. 3.

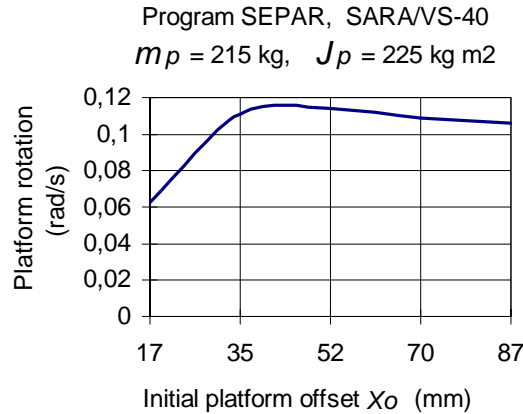


Figure 3 – Platform rotation after separation from rocket booster

As one can see, the rotation rate has its maximum value $\omega_p = 0.114$ rad/s, when the platform initial offset is 30 - 40 mm or skewing is of $\sim 1.7 - 2.3^\circ$. For values $x_0 > 40$ mm, the platform rotation decreases because of the springs pusher behavior decrease. This value ($\omega_p = 0.114$ rad/s) cannot be admitted for microgravity experiments (see charter 5). Hence, it is necessary to use a special guide during the platform separation or a restrainer after separation.

4. SIMULATION OF RESTRAINER OPERATING

The restrainer consists of a shredding cord with length l_R . The ends of the cord (Fig. 2c) are fixed on the platform (point A) and on the booster (point B). After the platform separation, the cord is tired apart, creating in this way a stabilizing force, Figure 2c, with relatively constant value F_R . The platform motion during the restrainer operating can be written in the form

$$m_p d^2 x_p / dt^2 = -F_R \quad (10)$$

$$J_p d \omega_p / dt = F_R l_R \sin \alpha_p \quad (11)$$

The simulation of the restrainer operating for SARA platform with use of RESTR program is calculated for initial flight parameters, obtained in SEPAR program calculation: $\omega_p(0) = 0.114$ rad/s, $\omega_b(0) = 0.48$ rad/s, $dx_p/dt(0) = 0,3$ m/s, $dx_b/dt(0) = 0,32$ m/s, $\alpha_p(0) = 0.038$ rad, $\alpha_b(0) = 0.018$ rad, $x_p(0) = 12$ mm, $x_b(0) = 13$ mm. The result of the platform dynamic calculation, during the restrainer operating, for length $l_R = 10$ m and $F_R = 10$ N is shown in Fig. 4.

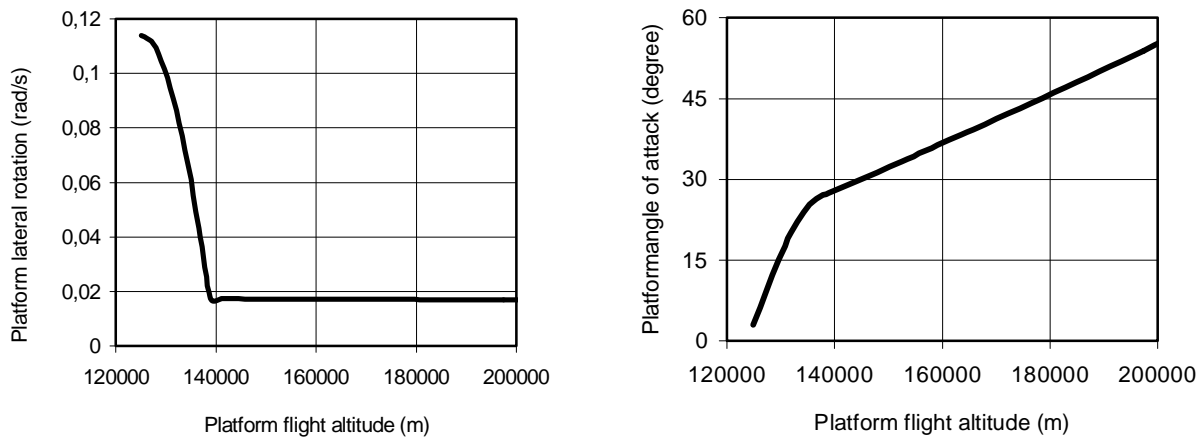


Figure 4 – Simulation of platform stabilization due to use of restrainer

During SARA platform flight from altitude of 125 km up to 140 km, its lateral rotation reduces from 0.114 rad/s up to 0.0153 rad/s (Fig.4). When the restrainer operating finishes, the platform rotation is constant.

5. MICROGRAVITY ENVIRONMENT

One can determine the platform rotation value for microgravity experiments during its outer atmosphere flight, as it is possible to calculate the dimensionless centripetal acceleration G_m (Fig. 5).

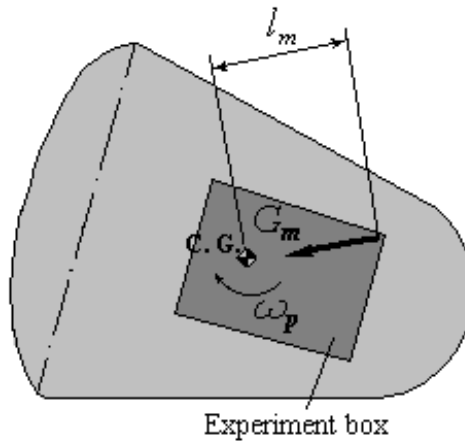


Figure 5 – Scheme of microgravity load in the platform experiment box

$$G_m = a_m/g = l_m \omega_p^2/g \quad (12)$$

where a_m centripetal acceleration, m/s^2
 l_m maximum distance from platform centre of gravity to experiment equipment, m
 g gravity acceleration, m/s^2 .

Figure 6 shows the calculation results of microgravity load for SARA platform as the function of dimensionless acceleration G_m versus initial platform angle of offset $\alpha_0 = \arctg(x_0/2R)$ for distance $l_m = 0.4$ m.

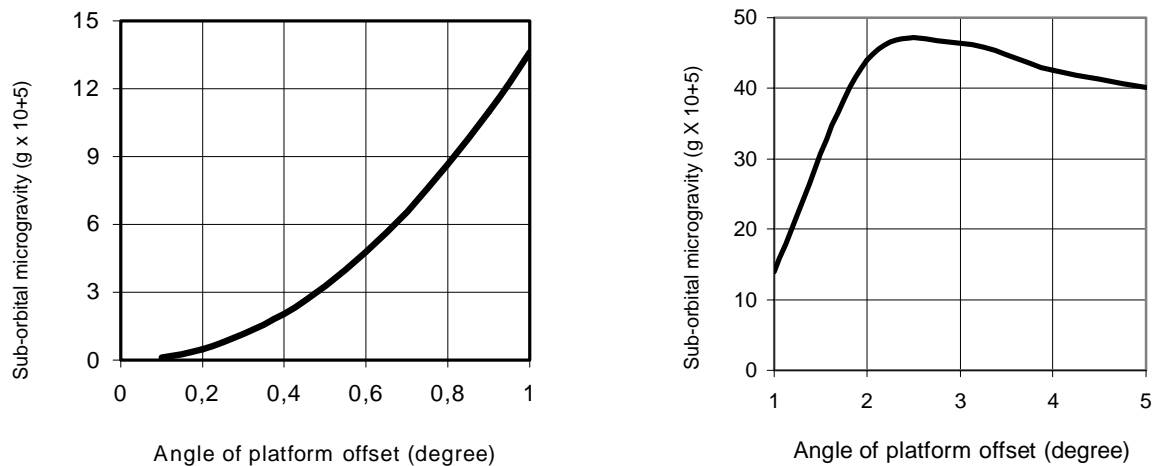


Figure 6 – Microgravity load in the experiment box during the flight in the outer atmosphere

As follows from Fig. 6, in order to guaranty value $G_m < 10^{-5}$ without restrainer, it is necessary to provide the platform initial angle $\alpha_0 < 0.25^\circ$ and for $G_m < 10^{-4}$ the angle $\alpha_0 < 0.9^\circ$. If the platform offset angle is $\alpha_0 \sim 2^\circ$ it is possible the maximum microgravity level of $G_m > 0.4 \cdot 10^{-3}$ (Fig. 6).

With the use of the restrainer for SARA platform, the maximum value of microgravity dimensionless acceleration is $G_m = 10^{-5}$ (for rate of rotation $\omega_p = 0.0153$ rad/s). For restrainer force $F_R = 40$ N it is possible to reduce the platform rate of rotation up to $\omega_p \sim 0.005$ rad/s and, correspondingly, from formula (12), the reducing of microgravity level up to $G_m \sim 10^{-6}$.

6. ATMOSPHERIC RE-ENTRY

At the beginning of the atmospheric re-entry, at altitudes of approximately from 100 km up to 50 km it is possible to ignore the forces and moments caused by the platform rotation because of insignificant, in aerodynamic sense, values of the rotation rate and air density. Hence, in this case, the dynamics of the platform deceleration and rotation around its centre of gravity can be written (Koldaev, Guimaraes & Moraes, 1999)

$$m_p dV_p/dt = m_g g \sin \theta - C_D(\alpha_p, M) \pi R^2 \rho(H) V_p^2 / 2 \quad (13)$$

$$J_p d\alpha_p/dt = C_m(\alpha_p, M) \pi R^2 l \rho(H) V_p^2 / 2 \quad (14)$$

$$d\theta/dt = -g \cos \theta / V_p \quad (15)$$

where V_p platform velocity, m/s
 $\rho(H)$ air density, kg/m³
 R platform radius, m
 l platform characteristics length, m
 C_D platform drag coefficient
 C_m platform moment coefficient
 θ angle of trajectory, rad.

Air density versus flight altitude can approximately be calculated as, (Yaroshevskiy, 1988)

$$\rho(H) = \rho_0 e^{-\gamma(H-H^*)} \quad (16)$$

where H^* characteristic altitude (usually $H^* = 45$ km), m
 ρ_0 air density at characteristic altitude, kg/m³
 γ atmosphere parameter, 1/m.

Values of coefficients C_D and C_m are thought to be given as function of the platform angle of attack and Mach number of flight $M = V_p / \alpha(H)$, where $\alpha(H)$ is the sound velocity versus flight altitude. In the case when α_p is small and $M < 1$, then, the moment coefficients of the platform can be determined

$$C_m(\alpha_p) = (dC_y/d\alpha_p) \alpha_p (x_{pr} - x_c) / l \quad (17)$$

where C_y lateral force coefficient
 x_{pr} position of the center of pressure from platform nose, m
 x_c position of center of gravity, m

For large values of α_p and Mach number, the coefficients C_D and C_y one can calculate with the help of the known method for axisymmetric bodies, (Krasnov, 1989).

The flight dynamics of SARA platform at altitudes from 100 km up to 50 km is simulated by use of ENTRY program for rate of rotation $\omega_p = 0.0153$ rad/s, $dC_y/d\alpha_p = 1.25$, $(x_{pr} - x_c) = 0.363$ m and $l = 1.75$ m.

Figure 7 shows the simulation of the platform turning during its descent in the upper atmosphere with initial angles of attack 60°, 120° and 180°.

As one can see, in the course of the platform descent from altitude of 96 km during maximum 25-30 s the lateral rotation is transformed into the platform oscillation.

The oscillation amplitude has values from 10° up to 90° and depends on the initial angle of attack at the moment of the platform re-entry in the atmosphere (Fig. 7).

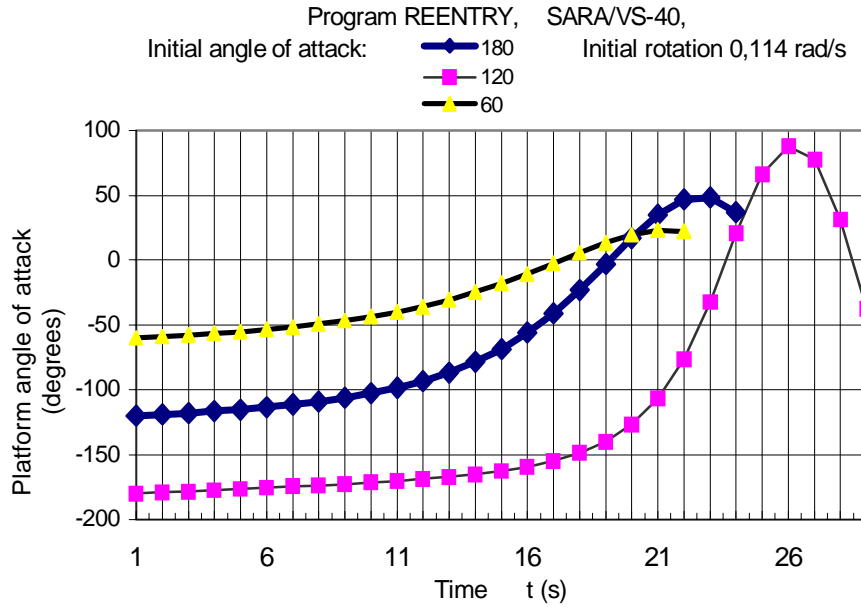


Figure 7 – Simulation of platform flight dynamics at altitudes 96-50 km

7. PLATFORM STABILIZATION IN LOWER ATMOSPHERE

In the lower atmosphere the influence of the platform rotation over its dynamics is considerable. In this case the equation for the platform angle of attack takes the form

$$J_p d^2 \alpha_p / dt^2 = [C_m(\alpha_p, \omega_p, M) + (dC_m / d\omega_p) d\omega_p / dt] \pi R^2 l \rho(H) V_p^2 / 2 \quad (18)$$

For the dimensionless rotation

$$(dC_m / d\omega_p) = (dm_z / O_z^*) l / V_p, \quad O_z^* = \omega_p l / V_p \quad (19)$$

The solution of equation (18) for the limited oscillation amplitude with constant angle of trajectory θ (Yaroshevskiy, 1988), is

$$\alpha_a = \omega_p / V_0 (4 J_p / (\gamma^2 \sin^2 \theta C_m \rho \pi R^2 l))^{1/4} e^{-\beta}$$

$$\beta = \rho \pi R^2 (dC_y / d\alpha_p - C_D - (dC_m / dO_z^* m_p l^2 / J_p) / (4 \gamma m_p \sin \theta)) \quad (20)$$

If one takes platform velocity, V_0 , as the solution of equation (13) for equation (20) and angle θ from equation (13), it is possible to approximately determine the value of amplitude α_p for each step of motion (program STAB).

Figure 8 shows the dynamics of SARA platform stabilization during its descent from altitude of 50 km up to 6 km with initial amplitude of platform oscillation α_a calculated with the help of the ENTRY program.

As it follows from Fig. 8, the time of platform stabilization for the moment coefficient derivative $dm_z / dO_z^* = 0.1$ is not more than 60 s.

So, in the absence of wind influence, at the moment of the parachute system deployment the SARA platform has a guaranteed stable motion with angle of attack not more than 10° .

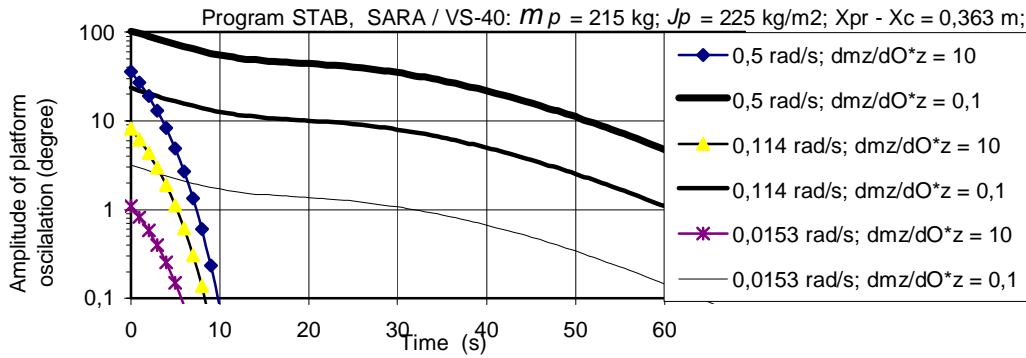


Figure 8 – Simulation of platform flight dynamics at altitudes 50 - 6 km

The function of lateral acceleration of the platform, G_l , versus time, given in Fig. 9, was calculated using the formula

$$G_l = C_y(\alpha_p) \pi R^2 \rho(H) V_p^2 / 2g \quad (21)$$

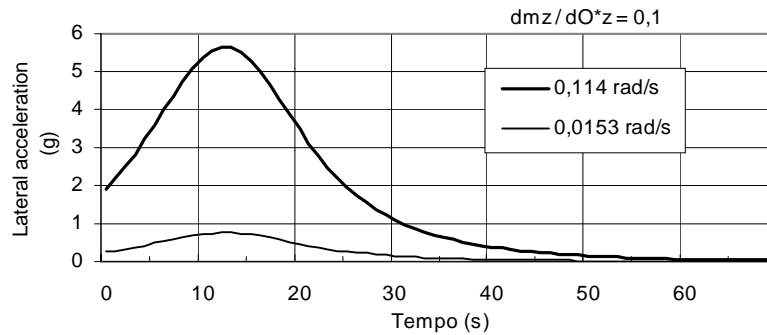


Figure 9 – Calculation of platform lateral acceleration at altitudes 50 - 6 km

The significant value of $G_l > 5g$ is explained by the presence of great angles of attack during the acting of maximum dynamic pressure $(\rho V_p^2 / 2)_{max}$.

8. FLIGHT DYNAMICS OF PLATFORM WITH PARACHUTE

The recovery system deployment and the platform flight with the parachute take place at subsonic velocity with relatively small angles of attack. Within this, the aerodynamic characteristics of the platform and the parachutes do not depend on Mach number. The system dynamics is described by equations analogous to (13) – (15) with the supplement of parachute force and moment (Koldaev, Guimaraes & Moraes, 1999).

The program TRAJDIN for the solution of these equations is available to do it. The dynamics simulation of SARA platform-parachute system is done for the following parameters: initial velocity $V_{p0} = 135$ m/s, $\alpha_{p0} = 10^\circ$, $\theta = 90^\circ$, $C_{D\alpha} = 0.55$, $S_d = 4$ m², $H_0 = 6$ km, $C_{Dp} = 0.8$, $S_p = 40$ m², $H_p = 4.5$ km. The result of the system dynamics at altitudes from 6 km up to 0 km is presented in Fig. 10. During 27 s the platform with the drag parachute decelerates to a velocity of 45 m/s. After the main parachute opening at altitude $H_p = 4.5$ km, the system velocity is reduced up to 10 - 12 m/s.

One should taken into account the small initial angle of attack and the great value of parachute moment, acting over the platform, and the time of the system stabilization is not more than 5 s.

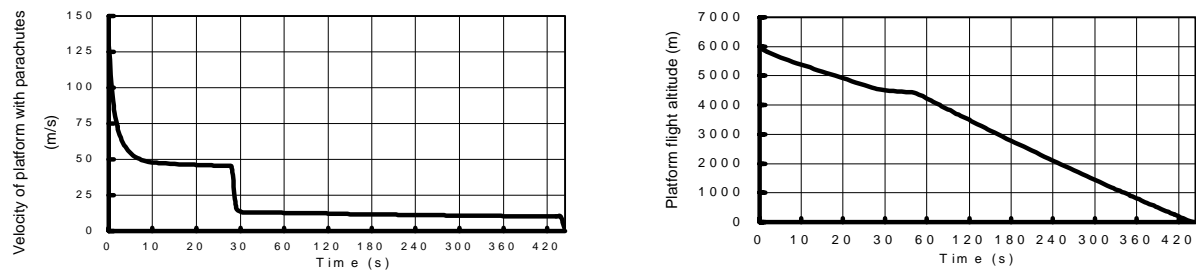


Figure 10 – Dynamics of SARA platform with parachutes (Program TRAJDIN)

8. CONCLUSION

The recoverable platform dynamics during its separation from the last rocket booster, sub-orbital flight, atmosphere re-entry, stabilization and descent with parachute have been modeled and simulated.

The application of VS-40 actuators for SARA platform separation can cause the rotation value, which is non-approved for microgravity experiments.

Use of a simple restrainer after the separation reduces significantly the platform rotation and guarantees microgravity environment during the sub-orbital flight.

The great angles of attack during re-entry during the platform stabilization in the atmosphere can cause significant lateral acceleration.

Use of drag and main parachutes provide stabilization and deceleration of the platform with the required parameters.

Acknowledgements

The first author would like to express his gratitude to CNPq for supporting him as visiting scientist (Grant No. 300.186/96-7) at the Space Systems Division of the Instituto de Aeronáutica e Espaço, Centro Técnico Aeroespacial.

9. REFERENCES

- Babuska, I., Práger, M., Vitásek, E., 1966, Numerical Process in Differential Equation, SNTL-Publishers of Technical Literature, Prague.
- Deweese, J., H., Schultz, E., R. & Nutt, A., B., 1978, Recovery System Design Guide, Technical Report, AFFDL-TR-78-151, Ca, USA.
- Koldaev, V., Guimarães, M., Moraes, P.Jr., 1999, Simulation of Parachute Dynamics, XV Congresso Brasileiro de Engenharia Mecânica, Águas de Lindoia-SP.
- Krasnov, 1989, Aerodynamics of Rocket, Mashinostroenie, Moscow.
- Moraes, P., Jr., 1998, Design Aspects of the Recoverable Orbital Platform SARA, 8º Congreso Chileno Ingenieria Me'ánica, Concepcion, Chile.
- Rysev, O., Ponomarev, A., Vasiliev, M., Vishniak, A., Dneprov, I., Mosseev, Y., 1996, Parachute Systems, "Nauka" publ. Co., Russian Academy of Science, Moscow.
- Fazolli, S., 1999, SARA Suborbital. Revisão Preliminar de Projeto, Relatório de revisões de projeto 021/GER-V/99, Cód. 587-320000/B7001, CTA/IAE, 1999
- Yaroshevsky, V. A., 1988, Reentry of space vehicles in atmosphere, Nauka, Moscow.